

**This is a self-archived version of an original article. This version may differ from the original in pagination and typographic details.**

**Author(s):** Wang, Youbao; Rinta-Antila, Sami; Dendooven, Peter; Huikari, Jussi; Jokinen, Ari; Kolhinen, Vesa; Lhersonneau, Gérard; Nieminen, Arto; Nummela, Saara; Penttilä, Heikki; Peräjärvi, Kari; Szerypo, Jerzy; Wang, Jicheng; Äystö, Juha

**Title:** Beta decay of neutron-rich 118Ag and 120Ag isotopes

**Year:** 2003

**Version:** Published version

**Copyright:** ©2003 American Physical Society

**Rights:** In Copyright

**Rights url:** <http://rightsstatements.org/page/InC/1.0/?language=en>

**Please cite the original version:**

Wang, Y., Rinta-Antila, S., Dendooven, P., Huikari, J., Jokinen, A., Kolhinen, V., Lhersonneau, G., Nieminen, A., Nummela, S., Penttilä, H., Peräjärvi, K., Szerypo, J., Wang, J., & Äystö, J. (2003). Beta decay of neutron-rich 118Ag and 120Ag isotopes. *Physical Review C*, 67(6), Article 064303. <https://doi.org/10.1103/PhysRevC.67.064303>

**$\beta$  decay of neutron-rich  $^{118}\text{Ag}$  and  $^{120}\text{Ag}$  isotopes**

Y. Wang, S. Rinta-Antila, P. Dendooven,\* J. Huikari, A. Jokinen,† V. S. Kolhinen, G. Lhersonneau,‡ A. Nieminen, S. Nummela,§ H. Penttilä, K. Peräjärvi,|| J. Szerypo,¶ J. C. Wang,\*\* and J. Äystö  
*Department of Physics, P.O. Box 35, FIN-40014 University of Jyväskylä, Finland*

(Received 12 September 2002; published 12 June 2003)

$\beta$  decays of on-line mass-separated neutron-rich  $^{118}\text{Ag}$  and  $^{120}\text{Ag}$  isotopes have been studied by using  $\beta$ - $\gamma$  and  $\gamma$ - $\gamma$  coincidence spectroscopy. Extended decay schemes to the  $^{118,120}\text{Cd}$  daughter nuclei have been constructed. The three-phonon quintuplet in  $^{118}\text{Cd}$  is completed by including a new level at 2023.0 keV, which is tentatively assigned the spin and parity of  $2_4^+$ . The intruder band in  $^{118}\text{Cd}$  is proposed up to the  $4^+$  level at 2322.4 keV. The measured  $\beta$ -decay half-life for the high-spin isomer of  $^{120}\text{Ag}$  is  $0.40 \pm 0.03$  s. Candidates for the three-phonon states, as well as the lowest members of the intruder band in  $^{120}\text{Cd}$ , are also presented. These data support the coexistence of quadrupole anharmonic vibration and proton particle-hole intruder excitations in  $^{118,120}\text{Cd}$ .

DOI: 10.1103/PhysRevC.67.064303

PACS number(s): 23.20.Lv, 23.40.Hc, 21.10.Re, 27.60.+j

**I. INTRODUCTION**

Even mass Cd nuclei have an interesting structure that is indicative of the coexistence of quadrupole anharmonic vibration and proton particle-hole intruder excitations. According to the spherical quadrupole vibrator model [1], a perfect vibrator would present sets of equally spaced, degenerate phonon states between which one-phonon jump transitions are allowed as electric quadrupole transitions. The splitting among the members of the phonon multiplet can be accounted for by introducing anharmonic terms [2,3]. Indeed, intact anharmonic multiphonon excitations up to four quadrupole-phonon states have been identified in Cd nuclei [4–10]. With the analysis of the energy spectra of 26 nuclei presenting a vibrational structure, Kern *et al.* conclude that the Cd nuclei are among the best candidates for an anharmonic vibrator or a U(5) symmetry [11]. Proton two-particle two-hole excitations across the  $Z=50$  shell gap were introduced by Heyde *et al.* [12] in order to interpret the low-lying extra  $0^+$  and  $2^+$  states observed in  $^{112}\text{Cd}$  and  $^{114}\text{Cd}$  near the energies of the two-phonon triplet. It is shown that the above quintuplet of levels in  $^{112}\text{Cd}$  and  $^{114}\text{Cd}$  can be explained as a mixing of the normal quadrupole two-phonon excitation with proton  $2p$ - $2h$  intruder excitations. Since then, this configuration mixing scheme has been adopted in a number of in-

vestigations on Cd nuclei [5,13–17]. Experimentally, the ( $^3\text{He},n$ ) two-proton transfer reaction measurements on  $^{108}\text{Pd}$  and  $^{110}\text{Pd}$  targets have shown the evidence of proton-pair excitations across the major shell gap [18]. Rotationlike intruder bands have been reported in doubly even  $^{110-116}\text{Cd}$  [5,16,19,20], and a systematics has been built [20–22].

The level structures of more neutron-rich Cd nuclei are yet incompletely known; so far, the available information has been obtained uniquely from fission experiments. For  $^{118}\text{Cd}$  and  $^{120}\text{Cd}$ , yrast band up to a  $16^+$  level has been observed by prompt fission fragment spectroscopy [23–25].  $\beta$  decay of on-line mass-separated  $^{118}\text{Ag}$  and  $^{120}\text{Ag}$  sources produced by neutron-induced fission has been studied by several groups [8,13,26–29]. Decay half-lives,  $Q_\beta$  values, as well as decay schemes were reported. The bulk information on  $^{118}\text{Cd}$  and  $^{120}\text{Cd}$  nuclei has been provided via  $\beta^-$  decay of Ag parents [8,13,29], based on which  $^{118}\text{Cd}$  was interpreted as the first candidate for a perfect vibrator [8]. However, level lifetime measurements in  $^{116,118,120}\text{Cd}$  suggest discrepancies concerning the excited  $0^+$  states [30]. In addition, it is unclear whether the 1915.8 keV  $2_3^+$  level in  $^{118}\text{Cd}$  is a member of the three-phonon quintuplet [8] or a  $2^+$  intruder state as suggested in Refs. [20,22]. The aim of this paper is thus to provide new experimental data on  $^{118}\text{Cd}$  and  $^{120}\text{Cd}$ . These data were obtained from the decay of on-line mass-separated Ag sources that were produced by proton-induced symmetric fission and ion-guide technique. This method is very effective in producing the neutron-rich isotopes at this mass region [31]. The low-lying level structure of  $^{118}\text{Cd}$  and  $^{120}\text{Cd}$  with addition of new identified states are discussed in the context of coexistence of quadrupole anharmonic vibration and intruder excitations.

**II. EXPERIMENT**

The measurements were carried out at the ion-guide isotope separator on-line facility [32–34] of the University of Jyväskylä. Symmetric fission of natural uranium induced by 25 MeV protons was applied for the production of  $^{118}\text{Ag}$  and  $^{120}\text{Ag}$  sources. The proton beam intensity used in the experi-

\*Present address: KVI, Zernikelaan 25, NL-9747 AA, Groningen, The Netherlands.

†Present address: EP-ISOLDE, CERN, CH-1211, Geneva, Switzerland.

‡Present address: INFN, Laboratori Nazionali di Legnaro, Via Romea 4, I-35020 Legnaro, Italy.

§Present address: CERN, CH-1211, Geneva, Switzerland.

||Present address: EP-ISOLDE, CERN, CH-1211, Geneva, Switzerland.

¶Present address: Sektion Physik, University of Munich (LMU), D-85748 Garching, Germany.

\*\*Present address: Argonne National Laboratory, 9700 South Cass Avenue, Argonne, Illinois 60439, USA.

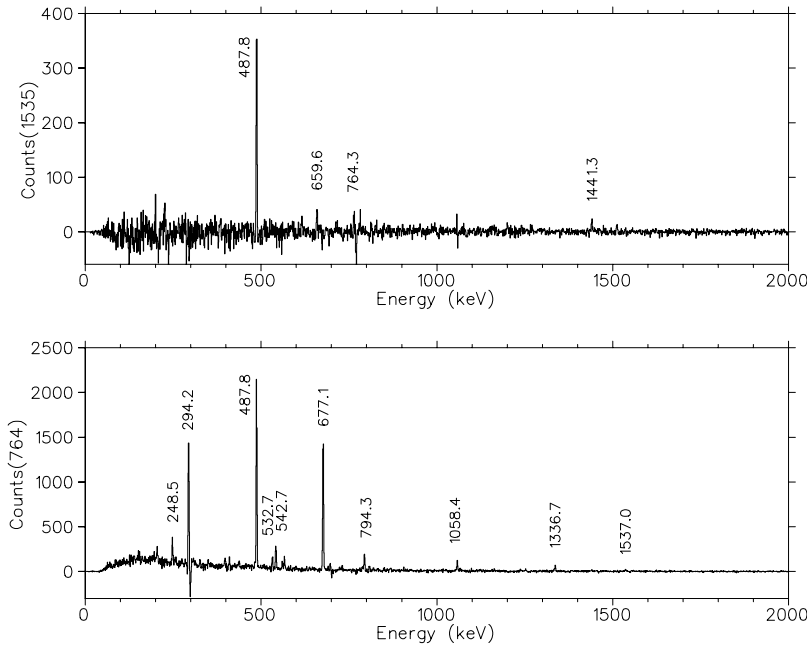


FIG. 1. Projections gated by the 1535 keV (top) and 764 keV (bottom) transitions of  $^{118}\text{Cd}$ . The weak peaks in the upper spectrum arise from another transition (1537.0 keV) placed between the levels at 3466.0 and 1929.1 keV. The upper spectrum implies a placement of the 1535.2 keV  $\gamma$  transition directly on top of the 487.8 keV  $2_1^+$  state, see text. The lower spectrum is useful for looking up the intensity of the 1537.0 keV transition. The 1058.4 keV peak is due to a very weak transition with energy close to the gate.

ments was about 5–10  $\mu\text{A}$ . Mass-separated beam was implanted into a movable tape situated in the center of a thin cylindrical plastic scintillator. The implantation point was viewed by four Ge detectors placed in close geometry. The experimental data were collected in  $\beta$ - $\gamma$  or  $\gamma$ - $\gamma$  coincidence modes, with the time stamping of events defined by the cycle of the tape movement. This experimental setup is very similar to our previous one, and a more detailed description can be found in Refs. [9,35].

There are two known  $\beta$ -decaying states in  $^{118}\text{Ag}$  and  $^{120}\text{Ag}$ , i.e., the low-spin ground state and a higher-spin isomer [26,36]. In the experiment both were produced as on-line sources from fission fragments. The average production rate for  $^{120}\text{Ag}^m$  [ $I^\pi=(6^-)$ ] is about 1750 ions/s. In the calculation  $^{120}\text{Ag}^m$  is assumed to be solely produced in fission,

and its  $\beta$ -decay branch ratio of 63% [26] has been considered. The ground state of  $^{120}\text{Ag}$  [ $I^\pi=(3^+)$ ] can be fed by  $\beta$  decay of doubly even  $^{120}\text{Pd}$  and by the  $E3$  isomeric transition from  $^{120}\text{Ag}^m$  [26]. The production rate for  $^{120}\text{Pd}$  is much lower than that of  $^{120}\text{Ag}$ , estimated to be below 100 ions/s, and its decay scheme is little known [37]. Therefore, an upper production limit of 2400 ions/s for  $^{120}\text{Ag}$  is obtained by assuming no feedings from  $^{120}\text{Pd}$ .

The construction of level schemes is based on  $\gamma$ - $\gamma$  coincidence relationships and coincidence rates. In the experiment for  $^{118}\text{Ag}$ , the short collection cycle suppressed the activities of the relatively long-lived ground state of  $^{118}\text{Ag}$  ( $T_{1/2}=3.76$  s). Nevertheless, many new  $\gamma$  transitions were assigned to the decay of the known isomer  $^{118}\text{Ag}^m$  ( $T_{1/2}=2.0$  s). In the case of  $^{120}\text{Ag}$ , separate decay schemes have

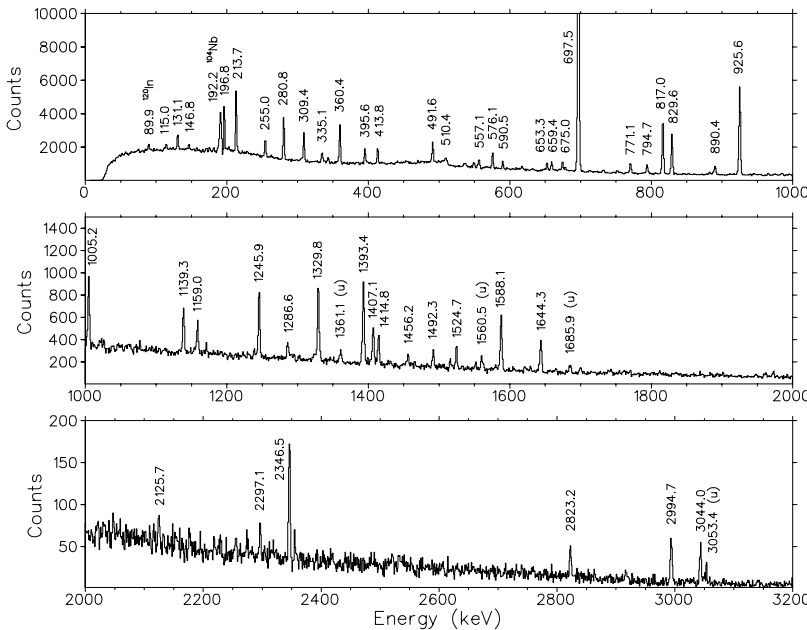


FIG. 2.  $\gamma$  spectrum gated by the 505.7 keV  $2_1^+ \rightarrow 0^+$  ground state transition of  $^{120}\text{Cd}$ . A few unplaced transitions of  $^{120}\text{Cd}$  are indicated by (u) following the energy. The 192.2 keV transition is from the  $\beta$  decay of  $^{104}\text{Nb}$  formed as monoxide ions ( $A+16$ ).

TABLE I. List of  $\gamma$  rays from the decay of  $^{118}\text{Ag}^m$ ; 100  $\gamma$  intensity units correspond to a  $\beta$  feeding of 97.8%. The intensities of the 487.8, 646.2, 781.7, 1269.5, and 1428.0 keV  $\gamma$  rays have been scaled such as to balance the population of the  $2^+$  states at 487.8, 1269.5, and 1915.8 keV without direct  $\beta$  feedings.

$E_\gamma$ (keV)	$I_\gamma$ (Rel.)	$E_i$ (keV)	$E_f$ (keV)	$I_i^\pi$	$I_f^\pi$	$E_\gamma$ (keV)	$I_\gamma$ (Rel.)	$E_i$ (keV)	$E_f$ (keV)	$I_i^\pi$	$I_f^\pi$
190.1 (2)	0.6 (1)	2662.0	2471.8		( $5_3^-$ )	771.0 (1)	22.3 (15)	1935.9	1164.9	$6^+$	$4_1^+$
209.6 (2)	0.6 (1)	3031.9	2822.4			781.7 (1)	3.3 (3)	1269.5	487.8	$2_2^+$	$2_1^+$
222.8 (2)	0.4 (1)	2978.8	2756.0			788.1 (1)	1.7 (1)	3260.0	2471.8		( $5_3^-$ )
230.9 (2)	0.7 (2)	2322.4	2091.6	( $4_3^+$ )	$3^+$	794.3 (1)	1.4 (1)	2723.4	1929.1		$4_2^+$
246.2 (1)	3.1 (4)	2182.1	1935.9	( $5_1^-$ )	$6^+$	798.0 (2)		1285.8	487.8	$0_2^+$	$2_1^+$
248.5 (1)	7.6 (8)	2471.8	2223.3	( $5_3^-$ )	( $5_2^-$ )	808.5 (1)	7.1 (5)	3031.9	2223.3		( $5_2^-$ )
258.5 (1)	2.4 (2)	3290.4	3031.9			820.2 (1)	1.0 (2)	2756.0	1935.9		$6^+$
275.9 (1)	3.8 (2)	3031.9	2756.0			822.1 (1)	0.7 (1)	2091.6	1269.5	$3^+$	$2_2^+$
294.2 (1)	3.1 (7)	2223.3	1929.1	( $5_2^-$ )	$4_2^+$	849.8 (1)	3.1 (4)	3031.9	2182.1		( $5_1^-$ )
307.5 (2)	0.3 (1)	2223.3	1915.8	( $5_2^-$ )	$2_3^+$	926.6 (2)	0.8 (1)	2091.6	1164.9	$3^+$	$4_1^+$
308.5 (2)	0.8 (2)	3031.9	2723.4			968.1 (1)	2.8 (2)	3290.4	2322.4		( $4_3^+$ )
313.9 (2)	1.3 (1)	2954.4	2640.6			1013.9 (2)	0.4 (1)	3237.1	2223.3		( $5_2^-$ )
336.3 (2)	0.5 (1)	3290.4	2954.4			1018.6 (1)	1.1 (1)	2954.4	1935.9		$6^+$
350.6 (1)	1.0 (2)	2822.4	2471.8		( $5_3^-$ )	1036.8 (2)	0.6 (1)	3260.0	2223.3		( $5_2^-$ )
369.8 (2)	0.7 (1)	3031.9	2662.0			1042.9 (1)	0.3 (1)	2978.8	1935.9		$6^+$
391.2 (1)	2.6 (2)	3031.9	2640.6			1058.4 (1)	37.0 (25)	2223.3	1164.9	( $5_2^-$ )	$4_1^+$
397.7 (1)	4.0 (2)	2621.0	2223.3		( $5_2^-$ )	1067.2 (1)	3.0 (2)	3290.4	2223.3		( $5_2^-$ )
406.6 (2)	0.8 (1)	2322.4	1915.8	( $4_3^+$ )	$2_3^+$	1095.9 (1)	3.5 (2)	3031.9	1935.9		$6^+$
411.0 (1)	2.7 (2)	3031.9	2621.0			1127.3 (3)		1615.1	487.8	$0_3^+$	$2_1^+$
433.6 (2)	1.8 (1)	2756.0	2322.4		( $4_3^+$ )	1157.4 (1)	4.0 (3)	2322.4	1164.9	( $4_3^+$ )	$4_1^+$
438.7 (1)	2.6 (2)	2662.0	2223.3		( $5_2^-$ )	1237.2 (2)	0.7 (2)	3460.4	2223.3		( $5_2^-$ )
468.0 (2)	1.2 (1)	3290.4	2822.4			1269.5 (1)	2.3 (2)	1269.5	0.0	$2_2^+$	$0_1^+$
474.0 (2)	0.4 (1)	3031.9	2557.6			1301.1 (2)	0.4 (1)	3237.1	1935.9		$6^+$
487.8 (1)	100.0	487.8	0.0	$2_1^+$	$0_1^+$	1306.9 (2)	0.5 (1)	2471.8	1164.9	( $5_3^-$ )	$4_1^+$
532.7 (1)	5.8 (4)	2756.0	2223.3		( $5_2^-$ )	1324.1 (2)	0.8 (1)	3260.0	1935.9		$6^+$
542.7 (1)	1.6 (2)	2471.8	1929.1	( $5_3^-$ )	$4_2^+$	1336.7 (2)	1.0 (1)	3265.8	1929.1		$4_2^+$
544.3 (2)	0.2 (1)	3290.4	2745.8			1392.7 (2)	0.9 (1)	2557.6	1164.9		$4_1^+$
560.0 (2)	3.6 (2)	3031.9	2471.8		( $5_3^-$ )	1411.1 (2)	1.1 (1)	3347.0	1935.9		$6^+$
567.1 (1)	1.7 (1)	3290.4	2723.4			1428.0 (1)	0.7 (1)	1915.8	487.8	$2_3^+$	$2_1^+$
583.9 (2)	0.6 (1)	3237.1	2653.0			1441.3 (1)	2.9 (2)	1929.1	487.8	$4_2^+$	$2_1^+$
598.0 (2)	0.7 (1)	3260.0	2662.0			1488.1 (2)	0.9 (1)	2653.0	1164.9		$4_1^+$
599.0 (1)	1.7 (2)	2822.4	2223.3		( $5_2^-$ )	1524.4 (2)	0.5 (1)	3460.4	1935.9		$6^+$
628.3 (2)	0.7 (1)	3290.4	2662.0			1535.2 (4)	0.3 (1)	2023.0	487.8	( $2_4^+$ )	$2_1^+$
646.2 (1)	0.4 (1)	1915.8	1269.5	$2_3^+$	$2_2^+$	1537.0 (4)	0.3 (1)	3466.0	1929.1		$4_2^+$
649.7 (2)	0.4 (1)	3290.4	2640.6			1547.4 (2)	0.5 (1)	3483.3	1935.9		$6^+$
659.6 (1)	4.5 (3)	1929.1	1269.5	$4_2^+$	$2_2^+$	1558.3 (3)	0.9 (1)	2723.4	1164.9		$4_1^+$
669.4 (2)	0.3 (1)	3290.4	2621.0			1580.9 (3)	1.3 (1)	2745.8	1164.9		$4_1^+$
677.1 (1)	88.5 (57)	1164.9	487.8	$4_1^+$	$2_1^+$	1585.9 (5)		2073.7	487.8	$0_4^+$	$2_1^+$
691.8 (1)	0.3 (1)	2621.0	1929.1		$4_2^+$	1603.7 (3)	1.4 (1)	2091.6	487.8	$3^+$	$2_1^+$
704.7 (1)	6.2 (4)	2640.6	1935.9		$6^+$	1735.5 (3)	0.2 (1)	2223.3	487.8	( $5_2^-$ )	$2_1^+$
717.1 (2)	0.7 (1)	2653.0	1935.9		$6^+$	1758.4 (3)	1.1 (1)	2923.3	1164.9		$4_1^+$
731.1 (1)	3.4 (4)	2954.4	2223.3		( $5_2^-$ )	2100.8 (4)	6.2 (4)	3265.8	1164.9		$4_1^+$
732.6 (2)	0.7 (1)	3290.4	2557.6			2163.7 (5)	3.1 (2)	3328.6	1164.9		$4_1^+$
755.5 (2)	0.5 (1)	2978.8	2223.3		( $5_2^-$ )	2777.8 (6)	2.1 (2)	3265.8	487.8		$2_1^+$
764.3 (1)	2.5 (2)	1929.1	1164.9	$4_2^+$	$4_1^+$						

been built for its ground state and higher-spin isomer, respectively. As an example, two  $\gamma$  spectra gated by the 1535 keV and 764 keV transitions of  $^{118}\text{Cd}$ , respectively, are shown in Fig. 1. A  $\gamma$  spectrum in coincidence with the 505.7 keV  $2_1^+ \rightarrow 0^+$  ground state transition of  $^{120}\text{Cd}$  is shown in Fig. 2.

### III. RESULTS

#### A. Decay of $^{118}\text{Ag}^m$

Transitions assigned to the  $^{118}\text{Ag}^m$  decay are listed in Table I. The populated  $^{118}\text{Cd}$  levels are listed in Table II. The

TABLE II. Levels in  $^{118}\text{Cd}$  populated in the decay of  $^{118}\text{Ag}^m$ . The  $\log ft$  values are calculated with  $Q_\beta=7.27$  MeV [28,29] and  $T_{1/2}=2.0$  s [38]. The typical error for  $\log ft$  is 0.1.

Energy (keV)	$\beta$ feeding (%)	$\log ft$	$I^\pi$
0.0			$0^+$
487.8 (1)			$2^+$
1164.9 (1)	6.8 (59)	6.2	$4^+$
1269.5 (1)			$2^+$
1915.8 (1)			$2^+$
1929.1 (1)	2.4 (9)	6.4	$4^+$
1935.9 (2)	3.3 (16)	6.2	$6^+$
2023.0 (4)			$(2^+)$
2091.6 (1)	2.1 (3)	6.4	$3^+$
2182.1 (2)			$(5^-)$
2223.3 (1)	3.1 (27)	6.1	$(5^-)$
2322.4 (1)	0.8 (4)	6.7	$(4^+)$
2471.8 (1)	2.7 (9)	6.1	$(5^-)$
2557.6 (2)			
2621.0 (1)	1.2 (3)	6.4	
2640.6 (2)	1.8 (5)	6.2	
2653.0 (2)	1.0 (2)	6.5	
2662.0 (1)	1.0 (3)	6.5	
2723.4 (1)			
2745.8 (3)	1.1 (2)	6.4	
2756.0 (1)	4.2 (7)	5.8	
2822.4 (1)	0.9 (3)	6.4	
2923.3 (3)	1.1 (1)	6.3	
2954.4 (1)	5.3 (7)	5.6	
2978.8 (1)	1.2 (2)	6.2	
3031.9 (1)	26.0 (30)	4.9	
3237.1 (1)	1.4 (2)	6.0	
3260.0 (1)	3.8 (5)	5.6	
3265.8 (2)	9.1 (11)	5.2	
3290.4 (1)	13.6 (16)	5.0	
3328.6 (5)	3.0 (4)	5.7	
3347.0 (3)	1.1 (1)	6.1	
3460.4 (2)	1.2 (2)	6.0	
3466.0 (4)			
3483.3 (3)	0.5 (1)	6.4	

decay scheme is shown in two parts up to the 3290.4 keV  $^{118}\text{Cd}$  level, as can be seen in Figs. 3 and 4. Contributions from the decay of the  $^{118}\text{Ag}$  ground state are not negligible, especially to the low-lying  $0^+$  and  $2^+$  levels in  $^{118}\text{Cd}$ . It is assumed that these  $0^+$  and  $2^+$  states are not directly fed in the  $^{118}\text{Ag}^m$  decay, depopulation of the  $2^+$  levels at 487.8, 1269.5 and 1915.8 keV is therefore scaled down to balance the  $\gamma$ -ray intensity flow. It is thus found that the  $^{118}\text{Ag}^m$  decay accounts for 85% of the intensity of the 487.8 keV  $2_1^+ \rightarrow 0^+$  transition. The higher-lying  $^{118}\text{Cd}$  levels decay by transitions presumably of  $E1, M1/E2$  multipolarities to the low-lying  $4^+$ ,  $6^+$ , and  $5^-$  states; their population is consistent with the decay of  $^{118}\text{Ag}^m$  [(4)<sup>+</sup>].

Most levels in the decay scheme have been reported by Aprahamian and co-workers in Refs. [8,13,29]. Our data

confirm the former level scheme of  $^{118}\text{Cd}$  and allow for the addition of several new levels and their interpretations based on the systematics.  $\beta$  feedings and  $\log ft$  values are calculated as well under the assumption as aforementioned. In general, the decay properties of  $^{118}\text{Ag}^m$  are very similar to that of  $^{116}\text{Ag}^m$  [9]. This can be seen from the populated levels in  $^{118}\text{Cd}$  as well as their population strengths. Therefore one can compare the levels in these two Cd nuclei.

A new level at 2023.0 keV is identified by the transition of 1535.2 keV to the 487.8 keV  $2_1^+$  state, see Fig. 1. The 1535.2 keV transition was previously observed in Ref. [29], but not placed in the level scheme. The 1535.2 keV transition is influenced by the existence of another 1537.0 keV transition placed between the levels at 3466.0 and 1929.1 keV [29]. Nevertheless, the intensity of the 1535.2 keV transition can be obtained by looking up the difference between the total 1535 keV peak and the contribution of the 1537 keV transition seen from coincidence spectra, for example, in the gate of the 764 keV transition. It is found that the 1535.2 keV transition is less intense than previously observed in Ref. [29] by roughly a factor of 4. This might indicate that the 1535.2 keV transition is from the decay of  $^{118}\text{Ag}^g$ .

Previous studies have identified that the  $^{118}\text{Cd}$  levels at 1915.8, 1929.1, 1935.9, 2073.7, and 2091.6 keV are the  $2^+$ ,  $4^+$ ,  $6^+$ ,  $0^+$ , and  $3^+$  states, respectively. The  $2_4^+$  and  $3^-$  states are missing comparing with the known states in  $^{116}\text{Cd}$  at this excitation energies. In the decay of  $^{116}\text{Ag}^m$ , a 1951.4 keV  $2_4^+$  state in  $^{116}\text{Cd}$  is weakly populated, only one decay branch to the 513.5 keV  $2_1^+$  state is observed, while the  $3^-$  state at 1921.8 keV has another strong decay branch to the 1213.1 keV  $2_2^+$  state [9]. Therefore the new 2023.0 keV level in  $^{118}\text{Cd}$  appears more probable as the  $2_4^+$  state rather than the  $3^-$  state.

Several  $5^-$  bandheads are known in  $^{116}\text{Cd}$  [39,40], these  $5^-$  states are also populated in  $\beta^-$  decay of  $^{116}\text{Ag}^m$ , i.e., the 2249.1, 2292.3, and 2504.1 keV levels. The previously known 2223.3, 2182.1, and 2471.8 keV levels in  $^{118}\text{Cd}$  might correspond to the above mentioned  $5^-$  states in  $^{116}\text{Cd}$ , respectively, by their very similar decay properties. Direct  $\beta$  feedings to these levels are very small, supporting an even parity for  $^{118}\text{Ag}^m$ . In addition, several new transitions are placed as decaying from the 3031.9 and 3290.4 keV levels, which makes it more evident that these two levels are the most strongly fed ones in this decay. The  $\log ft$  values of 4.9 and 5.0, respectively, indicate allowed  $\beta$  transitions that might be associated with the fast  $\nu g_{7/2} \rightarrow \pi g_{9/2}$  Gamow-Teller (GT) transition.

The decay parent  $^{118}\text{Ag}^m$  was tentatively assigned as a  $4^+$  state, which also decays to the  $^{118}\text{Ag}$  ( $1^-$ ) ground state by an  $E3$  isomeric transition [26,38]. The weak but visible direct feedings to the excited  $0^+$  states in  $^{118}\text{Cd}$  by the decay of  $^{118}\text{Ag}^g$  appears in consistency with this assignment, but  $5^+$  may also be possible from the population of the  $6^+$   $^{118}\text{Cd}$  level as well as from the similarity comparing with the decay of  $^{116}\text{Ag}^m$ . We also note that in the  $\beta$  decay of  $^{118}\text{Pd}$ , the  $^{118}\text{Ag}$  ground state was suggested as a  $2^-$  state [37].

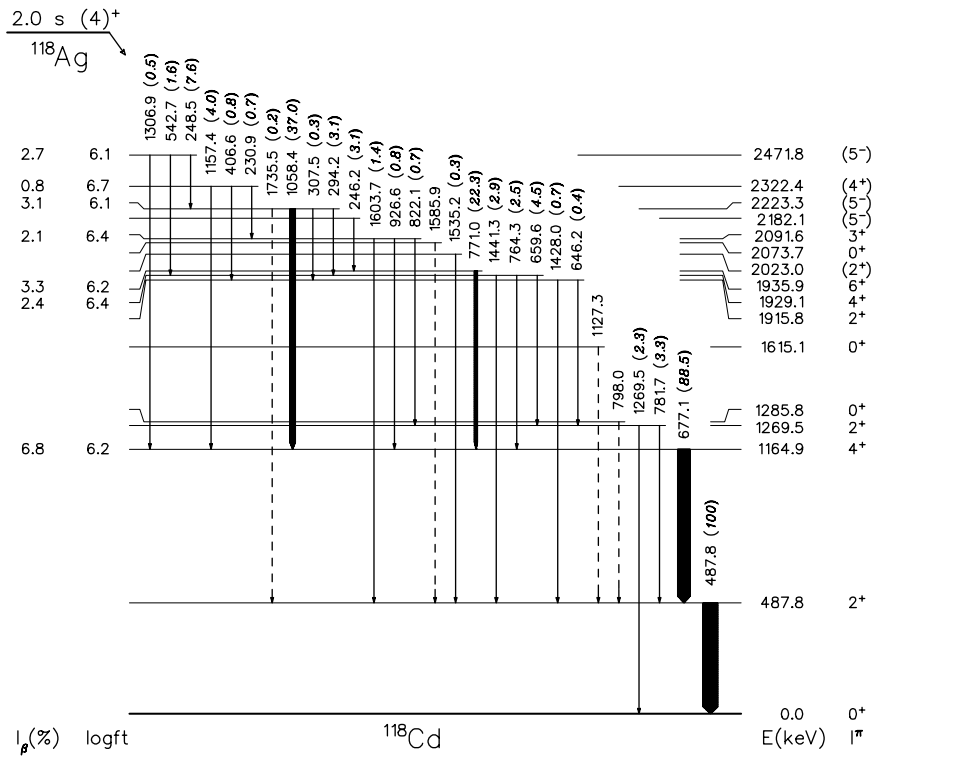


FIG. 3. Decay scheme of  $^{118}\text{Ag}^m$  (lower part). Dashed transitions are weak and only seen in the 487.8 keV gated spectrum. The excited  $0^+$  states in  $^{118}\text{Cd}$  are included for completeness.

**B. Decay of  $^{120}\text{Ag}$**

*1. Intensity ratios and decay half-lives*

In the experiment for  $^{120}\text{Ag}$ , one tape cycle contained collection and decay periods. To assign the  $^{120}\text{Cd}$  transitions to the decay of the two known  $^{120}\text{Ag}$  states, the peak areas of each transition during the decay and growth-in periods have been analyzed. These are shown in Fig. 5. In the figure,

transitions assigned to the decay of  $^{120}\text{Ag}^m$  can be recognized by the smallest ratios, while transitions belonging to the decay of  $^{120}\text{Ag}^g$  are indicated by larger ratios. Some transitions, for example, the 505.7 and 697.5 keV ones, are present in both decays; their ratios are therefore in between. The half-life of  $^{120}\text{Ag}^m$  was then analyzed from the most intense  $\gamma$  rays assigned to this decay. A weighted average of  $T_{1/2} = 0.40 \pm 0.03$  s was obtained. This is shown in Fig. 6 for

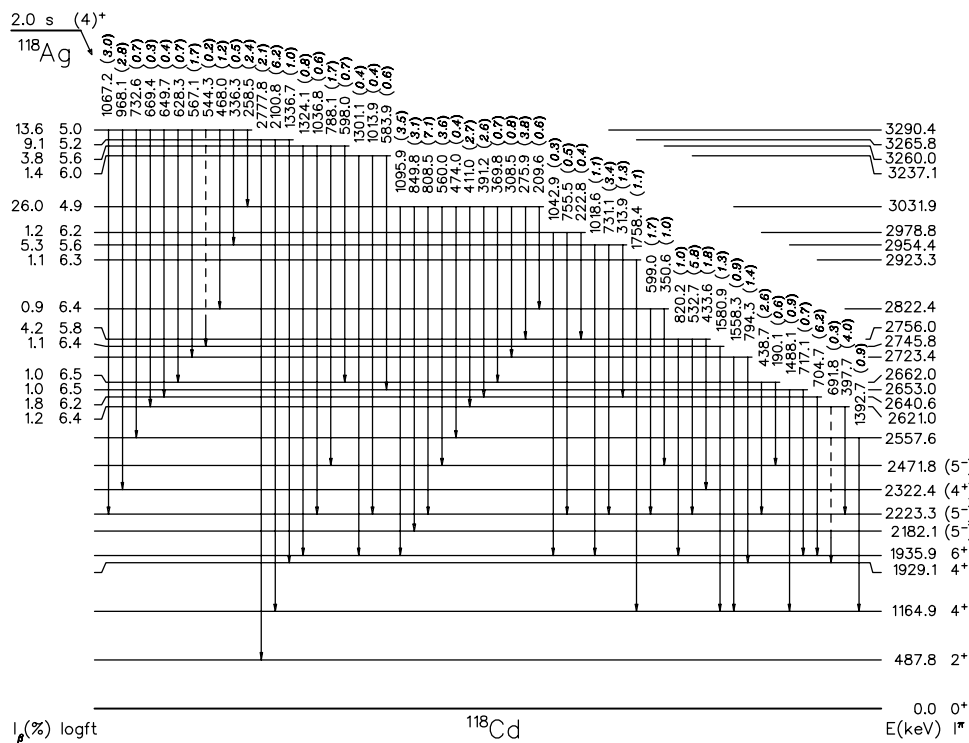


FIG. 4. Decay scheme of  $^{118}\text{Ag}^m$  (higher part).

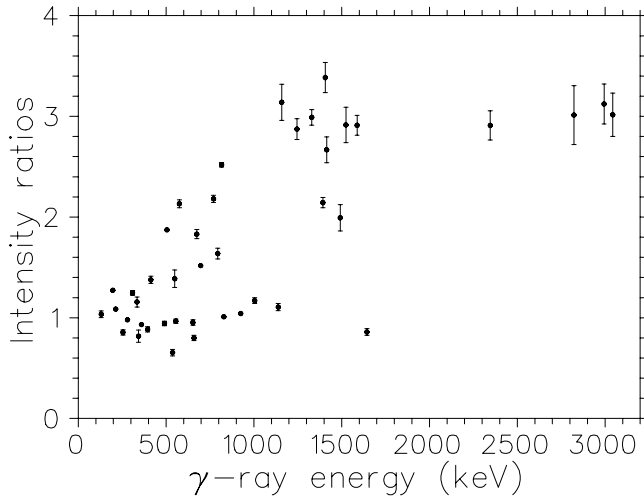


FIG. 5. Decay/growth intensity ratios for the transitions of  $^{120}\text{Cd}$ . The separator cycle was 1.7 s with collection during the first 0.7 s. The average ratio for the  $^{120}\text{Ag}^m$  parent activity (0.4 s) is calculated to be 1.1. For  $^{120}\text{Ag}^g$  this ratio is estimated to be about 1.7. The larger experimental ratios indeed indicate some long-lived components that do not agree with  $^{120}\text{Ag}^g$  (1.23 s) and  $^{120}\text{Pd}$  (0.5 s) [37], which might suggest another long-lived isomer in  $^{120}\text{Ag}$ . See text.

the 829.6 and 925.6 keV transitions. This value is larger than the previously reported 0.32(4) s [26,41]. For the ground state of  $^{120}\text{Ag}$ , the cycle length is inadequate for a reliable analysis of its half-life. We note that values of 1.17(5) s and 1.25(3) s have been reported by different groups [26,41,42], the evaluated half-life is  $1.23 \pm 0.03$  s [43].

## 2. Decay scheme of $^{120}\text{Ag}^g$

Transitions assigned to the decay of  $^{120}\text{Ag}^g$  are listed in Table III. The populated levels in  $^{120}\text{Cd}$  are listed in Table IV. The decay scheme is shown in Fig. 7. The present work confirms the former level scheme of  $^{120}\text{Cd}$  reported in Ref. [29] with addition of the upper four new levels. Tentative assignments of  $3^+$ ,  $2^+$ , and  $4^+$  to the levels at 1899.0, 1920.5, and 1997.9 keV, respectively, are based on systematics from  $^{116}\text{Cd}$  and  $^{118}\text{Cd}$ . The  $(2_3^+)$  state at 1920.5 keV

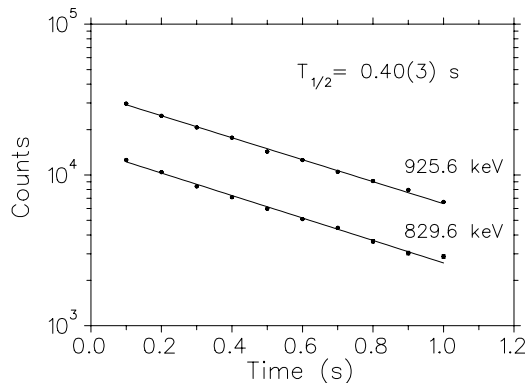


FIG. 6. Half-life of  $^{120}\text{Ag}^m$ .

TABLE III. List of  $\gamma$  rays from the decay of  $^{120}\text{Ag}^g$ . 100  $\gamma$  intensity units correspond to a  $\beta$  feeding of 93.0%.

$E_\gamma$ (keV)	$I_\gamma$ (Rel.)	$E_i$ (keV)	$E_f$ (keV)	$I_i^\pi$	$I_f^\pi$
442.0 (3)	0.3 (1)	2362.3	1920.5		$(2_3^+)$
505.7 (1)	100	505.7	0.0	$2_1^+$	$0_1^+$
549.7 (2)	1.5 (1)	2448.8	1899.0		$(3^+)$
576.1 (2)	3.0 (3)	1899.0	1322.8	$(3^+)$	$2_2^+$
675.0 (2)	2.6 (2)	1997.9	1322.8	$(4_2^+)$	$2_2^+$
697.5 (1)	41.7 (63)	1203.2	505.7	$4_1^+$	$2_1^+$
771.1 (2)	3.3 (6)	2093.8	1322.8	$2_4^+$	$2_2^+$
794.7 (2)	2.3 (2)	1997.9	1203.2	$(4_2^+)$	$4_1^+$
817.0 (1)	14.4 (11)	1322.8	505.7	$2_2^+$	$2_1^+$
882.9 (3)	0.8 (1)	1388.6	505.7	$0_2^+$	$2_1^+$
890.4 (2)	2.7 (2)	2093.8	1203.2	$2_4^+$	$4_1^+$
1039.4 (3)	0.4 (1)	2362.3	1322.8		$2_2^+$
1061.2 (4)	0.2 (1)	3423.6	2362.3		
1159.0 (3)	2.2 (2)	2362.3	1203.2		$4_1^+$
1238.8 (4)	0.4 (1)	1744.5	505.7	$0_3^+$	$2_1^+$
1245.9 (3)	5.1 (4)	2448.8	1203.2		$4_1^+$
1322.9 (2)	7.5 (8)	1322.8	0.0	$2_2^+$	$0_1^+$
1329.8 (3)	7.4 (6)	3423.6	2093.8		$2_4^+$
1393.4 (3)	4.9 (6)	1899.0	505.7	$(3^+)$	$2_1^+$
1407.1 (3)	3.6 (3)	3500.6	2093.8		$2_4^+$
1414.8 (3)	2.8 (2)	1920.5	505.7	$(2_3^+)$	$2_1^+$
1456.2 (3)	1.3 (2)	3549.9	2093.8		$2_4^+$
1492.3 (3)	1.8 (2)	1997.9	505.7	$(4_2^+)$	$2_1^+$
1524.7 (3)	2.6 (2)	3423.6	1899.0		$(3^+)$
1552.2 (4)	0.6 (1)	3549.9	1997.9		$(4_2^+)$
1588.1 (3)	7.1 (6)	2093.8	505.7	$2_4^+$	$2_1^+$
2100.7 (5)	0.8 (1)	3423.6	1322.8		$2_2^+$
2125.7 (5)	0.9 (1)	3328.9	1203.2		$4_1^+$
2178.1 (4)	1.4 (1)	3500.6	1322.8		$2_2^+$
2297.1 (4)	1.8 (2)	3500.6	1203.2		$4_1^+$
2346.5 (3)	6.8 (6)	3549.9	1203.2		$4_1^+$
2823.2 (4)	3.3 (3)	3328.9	505.7		$2_1^+$
2994.7 (4)	4.5 (4)	3500.6	505.7		$2_1^+$
3044.0 (4)	3.5 (3)	3549.9	505.7		$2_1^+$

appears to correspond to the  $(2_4^+)$  state in  $^{116}\text{Cd}$  and  $^{118}\text{Cd}$ . This  $2^+$  level in these three Cd nuclei is observed in  $\beta$  decay by a transition to the  $2_1^+$  state. The  $(3^+)$  state at 1899.0 keV decays to the first two  $2^+$  states, so does the  $(4_2^+)$  state at 1997.9 keV with another branch to the  $4_1^+$  state. These three  $^{120}\text{Cd}$  levels along with the 2032.8 keV  $6^+$  state are discussed in the following section as candidates of the three-phonon states. According to the quadrupole vibrator model, a  $0_4^+$  state is expected at this excitation energy region to form the complete set of three-phonon quintuplet. However, it is not observed in the present experiment. The  $0^+$  and  $2^+$  assignments to the 1744.5 and 2093.8 keV levels are from Ref. [29]. These two levels were presented as the lowest intruder states in Refs. [20,22].

Fogelberg *et al.* suggested a tentative assignment of  $3^+$  for the ground state of  $^{120}\text{Ag}$  [26]. The present work supports

TABLE IV. Levels in  $^{120}\text{Cd}$  populated in the decay of  $^{120}\text{Ag}^g$ . The  $\log ft$  values are calculated with  $Q_\beta=8.3$  MeV [28,29] and  $T_{1/2}=1.23$  s. The typical error for  $\log ft$  is 0.1.

Energy (keV)	$\beta$ feeding (%)	$\log ft$	$I^\pi$
0.0			$0^+$
505.7 (1)	13.9 (53)	6.1	$2^+$
1203.2 (1)	18.6 (50)	5.8	$4^+$
1322.8 (1)	9.7 (15)	6.1	$2^+$
1388.6 (3)	0.8 (1)	7.2	$0^+$
1744.5 (4)	0.4 (1)	7.4	$0^+$
1899.0 (2)	3.5 (7)	6.4	$(3^+)$
1920.5 (3)	2.4 (3)	6.5	$(2^+)$
1997.9 (2)	5.7 (6)	6.1	$(4^+)$
2093.8 (2)	0.7 (10)		$2^+$
2362.3 (2)	2.4 (3)	6.4	
2448.8 (2)	6.1 (6)	5.9	
3328.9 (3)	4.0 (5)	5.8	
3423.6 (2)	10.3 (10)	5.4	
3500.6 (2)	10.4 (10)	5.3	
3549.9 (2)	11.3 (11)	5.3	

this assignment by the observation of direct  $\beta$  feedings to the low-lying  $2_1^+$ ,  $4_1^+$ , and  $2_2^+$  levels. The spins for the  $^{120}\text{Cd}$  higher-lying new levels can be therefore limited to a range of 2–4 with an even parity according to the feedings.

3. Decay scheme of  $^{120}\text{Ag}^m$

Transitions assigned to the  $^{120}\text{Ag}^m$  decay are listed in Table V. The populated  $^{120}\text{Cd}$  levels are listed in Table VI.

The decay scheme is shown in Fig. 8. The feedings to the low-lying  $2_1^+$ ,  $4_1^+$ ,  $2_2^+$ , as well as to the  $(3^+)$  and  $(4_2^+)$  levels, are calculated by the balance of the  $\gamma$ -ray intensity flow, under assumption that these levels are only directly fed in the  $^{120}\text{Ag}$  ground state decay.

Several new  $^{120}\text{Cd}$  levels are identified and added in this decay scheme, including the strongly fed ones at 2686.1 and 3773.2 keV. The earlier observed  $^{120}\text{Cd}$  ground state band [23–25] is only weakly populated in the  $\beta^-$  decay up to  $(8^+)$  level at 2885.6 keV. Another  $(8^+)$  state at 2920.6 keV is also observed. The 2128.9 keV level is assumed as a  $5^-$  state by the intense transition of 925.6 keV to the  $4_1^+$  level, a similar transition in  $^{116}\text{Cd}$  and  $^{118}\text{Cd}$  has been observed from the 2249.1 and 2223.3 keV levels, respectively. The sizable feedings to the 2128.9 keV level are consistent with  $6^-$  for  $^{120}\text{Ag}^m$  that also decays to the  $^{120}\text{Ag}$  ground state by an E3 isomeric transition [26]. Unlike the decay of  $^{116}\text{Ag}^m$  and  $^{118}\text{Ag}^m$ , the  $^{120}\text{Ag}^m$  total decay strength is spread over more levels in  $^{120}\text{Cd}$ . The 2686.1 and 3773.2 keV  $^{120}\text{Cd}$  levels may have spins of 5–7 with odd parity, indicated by the allowed  $\beta$  transitions.

IV. DISCUSSION

The structure of even mass Cd nuclei has been well described in terms of configuration mixing of the quadrupole anharmonic vibration and intruder excitations [12]. Since the proton-neutron quadrupole interaction is primarily responsible for the excitation energies of intruder states, the resultant V-shape energy systematics of intruder states also reflects the degree of mixing of these two kinds of excitations. When

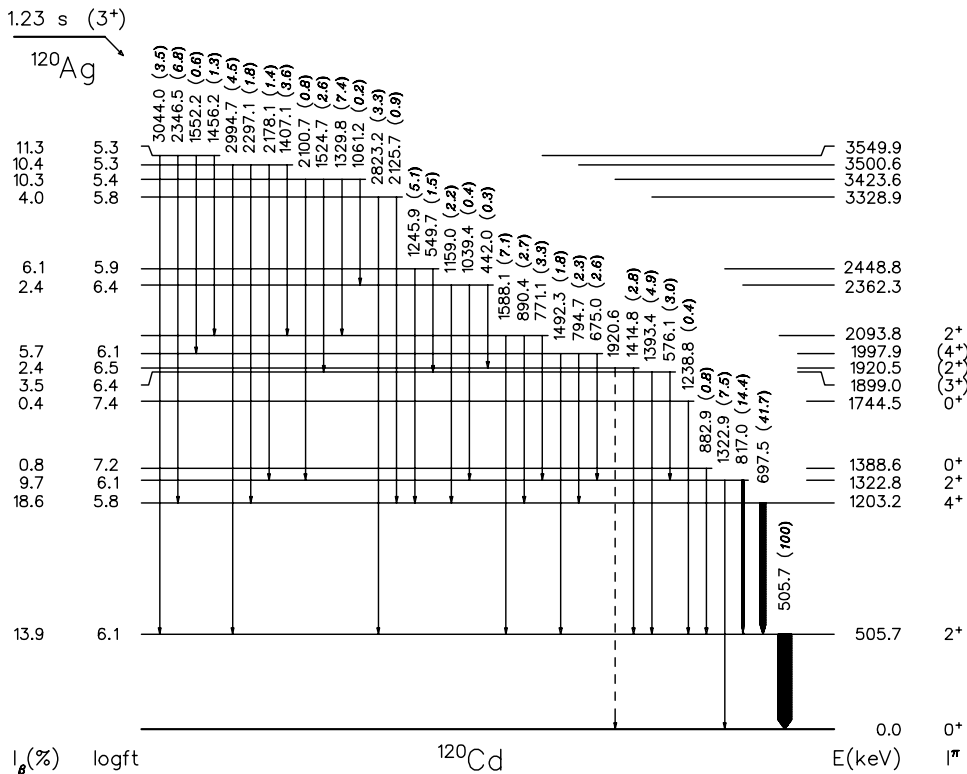


FIG. 7. Decay scheme of  $^{120}\text{Ag}^g$ . The dashed transition is regarded as tentative.



TABLE V. List of  $\gamma$  rays from the decay of  $^{120}\text{Ag}^m$ ; 100  $\gamma$  intensity units correspond to a  $\beta$  feeding of 98.6%.

$E_\gamma$ (keV)	$I_\gamma$ (Rel.)	$E_i$ (keV)	$E_f$ (keV)	$I_i^\pi$	$I_f^\pi$
115.0 (3)	0.7 (1)	2208.5	2093.8	(4 <sub>3</sub> <sup>+</sup> )	2 <sub>3</sub> <sup>+</sup>
131.1 (2)	1.9 (1)	2128.9	1997.9	(5 <sub>1</sub> <sup>-</sup> )	(4 <sub>2</sub> <sup>+</sup> )
146.8 (3)	0.6 (1)	2489.4	2342.5		
175.7 (2)	1.5 (2)	2208.5	2032.8	(4 <sub>3</sub> <sup>+</sup> )	6 <sup>+</sup>
182.2 (3)	0.9 (1)	2524.5	2342.5		
196.8 (2)	8.1 (5)	2686.1	2489.4		
213.7 (2)	8.0 (5)	2342.5	2128.9		(5 <sub>1</sub> <sup>-</sup> )
255.0 (2)	2.7 (2)	2779.5	2524.5		(4 <sub>3</sub> <sup>+</sup> )
280.8 (2)	7.8 (5)	2489.4	2208.5		(4 <sub>3</sub> <sup>+</sup> )
309.4 (2)	5.9 (4)	2208.5	1899.0	(4 <sub>3</sub> <sup>+</sup> )	(3 <sup>+</sup> )
335.1 (2)	2.2 (2)	2677.6	2342.5		
343.8 (2)	1.3 (1)	2686.1	2342.5		
360.4 (2)	8.0 (5)	2489.4	2128.9		(5 <sub>1</sub> <sup>-</sup> )
395.6 (2)	3.6 (2)	2524.5	2128.9		(5 <sub>1</sub> <sup>-</sup> )
413.8 (2)	4.1 (3)	2542.9	2128.9		(5 <sub>1</sub> <sup>-</sup> )
491.6 (2)	6.1 (4)	2524.5	2032.8		6 <sup>+</sup>
505.7 (1)	100	505.7	0.0	2 <sub>1</sub> <sup>+</sup>	0 <sub>1</sub> <sup>+</sup>
510.4 (2)	1.6 (2)	2542.9	2032.8		6 <sup>+</sup>
557.1 (2)	3.3 (3)	2686.1	2128.9		(5 <sub>1</sub> <sup>-</sup> )
576.1 (2)	3.2 (6)	1899.0	1322.8	(3 <sup>+</sup> )	2 <sub>2</sub> <sup>+</sup>
590.5 (2)	2.5 (2)	2489.4	1899.0		(3 <sup>+</sup> )
653.3 (2)	4.2 (3)	2686.1	2032.8		6 <sup>+</sup>
659.4 (2)	3.5 (3)	2788.3	2128.9		(5 <sub>1</sub> <sup>-</sup> )
675.0 (2)	0.8 (4)	1997.9	1322.8	(4 <sub>2</sub> <sup>+</sup> )	2 <sub>2</sub> <sup>+</sup>
697.5 (1)	91.3 (10.0)	1203.2	505.7	4 <sub>1</sub> <sup>+</sup>	2 <sub>1</sub> <sup>+</sup>
771.1 (2)	0.2 (1)	2093.8	1322.8	2 <sub>3</sub> <sup>+</sup>	2 <sub>2</sub> <sup>+</sup>
794.7 (2)	0.7 (2)	1997.9	1203.2	(4 <sub>2</sub> <sup>+</sup> )	4 <sub>1</sub> <sup>+</sup>
817.0 (1)	2.7 (6)	1322.8	505.7	2 <sub>2</sub> <sup>+</sup>	2 <sub>1</sub> <sup>+</sup>
829.6 (1)	20.4 (14)	2032.8	1203.2	6 <sup>+</sup>	4 <sub>1</sub> <sup>+</sup>
852.8 (3)	0.5 (1)	2885.6	2032.8	(8 <sub>1</sub> <sup>+</sup> )	6 <sup>+</sup>
887.8 (3)	0.8 (1)	2920.6	2032.8	(8 <sub>2</sub> <sup>+</sup> )	6 <sup>+</sup>
890.4 (2)	0.2 (1)	2093.8	1203.2	2 <sub>3</sub> <sup>+</sup>	4 <sub>1</sub> <sup>+</sup>
925.6 (1)	55.1 (38)	2128.9	1203.2	(5 <sub>1</sub> <sup>-</sup> )	4 <sub>1</sub> <sup>+</sup>
985.1 (2)	1.6 (2)	3773.2	2788.3		
1005.2 (2)	7.2 (5)	2208.5	1203.2	(4 <sub>3</sub> <sup>+</sup> )	4 <sub>1</sub> <sup>+</sup>
1139.3 (2)	5.8 (5)	2342.5	1203.2		4 <sub>1</sub> <sup>+</sup>
1230.1 (3)	1.1 (1)	3773.2	2542.9		
1286.6 (3)	2.0 (2)	2489.4	1203.2		4 <sub>1</sub> <sup>+</sup>
1322.9 (2)	1.4 (3)	1322.8	0.0	2 <sub>2</sub> <sup>+</sup>	0 <sub>1</sub> <sup>+</sup>
1393.4 (3)	5.1 (8)	1899.0	505.7	(3 <sup>+</sup> )	2 <sub>1</sub> <sup>+</sup>
1492.3 (3)	0.5 (2)	1997.9	505.7	(4 <sub>2</sub> <sup>+</sup> )	2 <sub>1</sub> <sup>+</sup>
1588.1 (3)	0.4 (2)	2093.8	505.7	2 <sub>3</sub> <sup>+</sup>	2 <sub>1</sub> <sup>+</sup>
1644.3 (3)	8.4 (7)	3773.2	2128.9		(5 <sub>1</sub> <sup>-</sup> )

moving from the neutron midshell, the excitation energies of the intruder states are expected to increase rapidly. This implies a possible distinct identification of these two families of excitations. In the neighboring  $^{116}\text{Cd}$  nucleus, the complete set of three-phonon quintuplet as well as the intruder band up to the 6<sup>+</sup> level have been identified [9,10,20]. A systematics of intruder levels in doubly even Cd nuclei has been built [20,22]. With compilation of the previous results, we discuss

TABLE VI. Levels in  $^{120}\text{Cd}$  populated in the decay of  $^{120}\text{Ag}^m$ . The  $\log ft$  values are calculated with  $Q_\beta=8.5$  MeV [28] and  $T_{1/2}=0.40$  s. The typical error for  $\log ft$  is 0.1.

Energy (keV)	$\beta$ feeding (%)	$\log ft$	$I^\pi$
0.0			0 <sup>+</sup>
505.7 (1)			2 <sup>+</sup>
1203.2 (1)			4 <sup>+</sup>
1322.8 (1)			2 <sup>+</sup>
1899.0 (2)			(3 <sup>+</sup> )
1997.9 (2)			(4 <sup>+</sup> )
2032.8 (2)	5.6 (17)	5.7	6 <sup>+</sup>
2093.8 (2)			2 <sup>+</sup>
2128.9 (1)	18.0 (42)	5.1	(5 <sup>-</sup> )
2208.5 (1)	7.3 (14)	5.5	(4 <sup>+</sup> )
2342.5 (2)	8.6 (15)	5.4	
2489.4 (1)	12.5 (21)	5.2	
2524.5 (2)	7.8 (13)	5.4	
2542.9 (3)	4.5 (8)	5.6	
2677.6 (3)	2.2 (4)	5.9	
2686.1 (1)	16.7 (26)	5.0	
2779.5 (3)	2.6 (4)	5.8	
2788.3 (3)	1.9 (4)	5.9	
2885.6 (4)	0.5 (1)	6.5	(8 <sup>+</sup> )
2920.6 (4)	0.8 (2)	6.3	(8 <sup>+</sup> )
3773.2 (2)	10.9 (18)	4.8	

the low-lying level structure of  $^{118}\text{Cd}$  and  $^{120}\text{Cd}$  in the context of coexistence of quadrupole anharmonic vibration and intruder excitations.

### A. Intruder states in $^{118}\text{Cd}$ and $^{120}\text{Cd}$

Systematics of the intruder states in doubly even Cd nuclei is shown in Fig. 9. In  $^{118}\text{Cd}$  it involves the 1615.1 keV  $0_3^+$  and 1915.8 keV  $2_3^+$  levels. The energy difference of 300 keV between these two levels agrees well with the systematic behavior. Although the  $2_3^+$  level was interpreted as a member of the three-phonon quintuplet in Ref. [8], the new 2023.0 keV ( $2_4^+$ ) state could be a substitute. Next, the intruder 4<sup>+</sup> state may have a large chance to be populated, provided that  $^{118}\text{Ag}^m$  has 4<sup>+</sup> or 5<sup>+</sup> character. It was demonstrated in the  $^{116}\text{Ag}^m$  decay that the  $^{116}\text{Cd}$  intruder 4<sup>+</sup> state at 2041.9 keV was weakly populated [9]. As the systematics shows, the intruder 4<sup>+</sup>-2<sup>+</sup> energy difference is roughly 400 keV, and an intraband  $E2$  transition is always observed. According to this behavior, the 2322.4 keV  $^{118}\text{Cd}$  level is a very suitable candidate for the 4<sup>+</sup> intruder state. The candidate level decays to the 1915.8 keV  $2_3^+$  state via a 406.6 keV transition, and also via the 1157.4 and 230.9 keV transitions to the 1164.9 keV  $4_1^+$  and 2091.6 keV  $3^+$  states, respectively. In addition, the 2322.4 keV level is fed from two higher-lying levels at 2756.0 and 3290.4 keV as shown in the decay scheme.

In the case of  $^{120}\text{Cd}$ , the 1744.5 keV  $0_3^+$  and 2093.8 keV  $2_4^+$  states are included in this intruder systematics. The spins

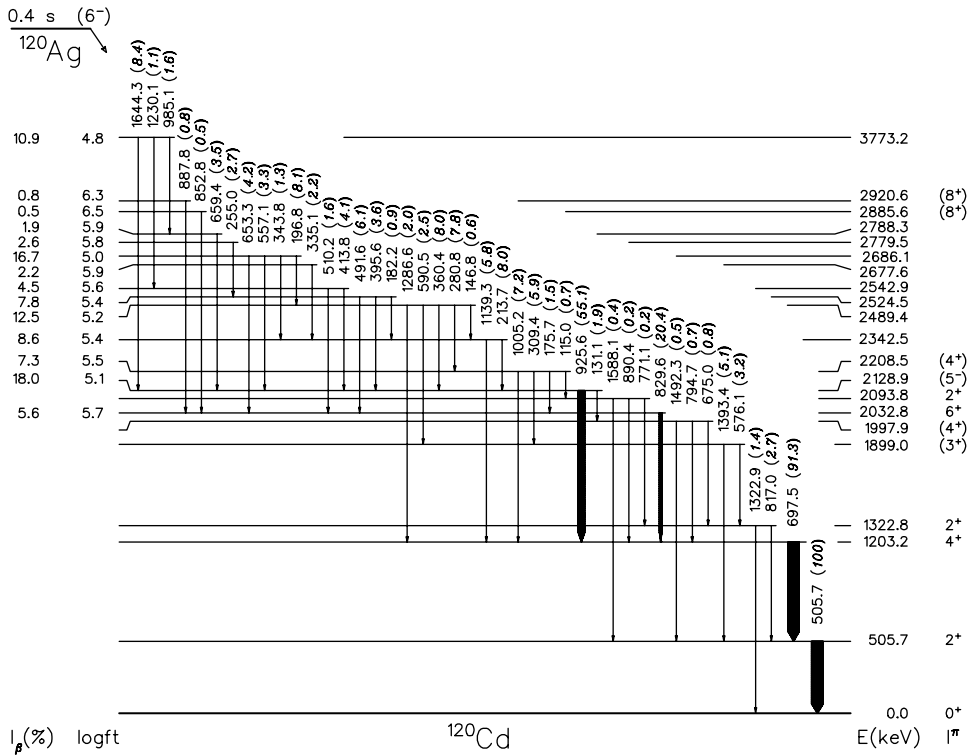


FIG. 8. Decay scheme of  $^{120}\text{Ag}^m$ .

of these two levels have been determined in Ref. [29]. In the present work, these two levels are populated in the  $^{120}\text{Ag}$  ground state decay. In general,  $\beta$  transitions to the intruder states are slow. This might be due to the very different configurations of the involved states.

**B. The three-phonon states in  $^{118}\text{Cd}$  and  $^{120}\text{Cd}$**

Aprahamian *et al.* suggested that the 1915.8, 1929.1, 1935.9, 2073.7, and 2091.6 keV levels form a complete set of three-phonon quintuplet of  $2^+$ ,  $4^+$ ,  $6^+$ ,  $0^+$ , and  $3^+$  states [8]. The present work modifies this interpretation only by the substitution of the 1915.8 keV  $2_3^+$  state with the new 2023.0 keV ( $2_4^+$ ) state in accordance with the intruder systematics.

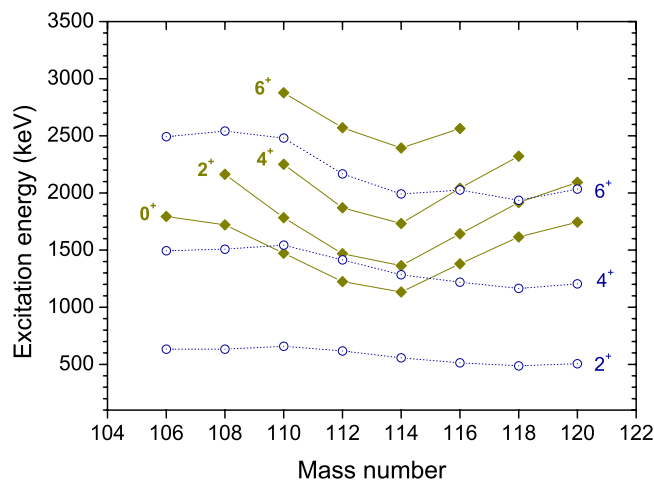


FIG. 9. Systematics of the intruder states in Cd nuclei. Yrast  $2^+, 4^+, 6^+$  states are shown for comparison.

One important character of the quadrupole three-phonon states is the preferred one-phonon decay to the  $N=2$  states by  $E2$  transitions. This can be tested by the  $B(E2)$  ratios, as were presented in Ref. [8] for  $^{118}\text{Cd}$ . For example, the 1929.1 keV  $4_2^+$  state has three decay branches to one-phonon  $2_1^+$  state and two-phonon  $4_1^+$ ,  $2_2^+$  states. The  $B(E2; 4_2^+ \rightarrow 2_2^+)/B(E2; 4_2^+ \rightarrow 2_1^+)$  ratio is 78 according to their relative intensities of these two  $E2$  transitions. This value is smaller than that in Ref. [8] of 100 but still clearly shows the dominance of  $\Delta N=1$ . For the 2091.6 keV  $3^+$  state, the  $B(E2; 3^+ \rightarrow 2_2^+)/B(E2; 3^+ \rightarrow 2_1^+)$  ratio is 15 if both transitions are pure  $E2$ . With correction of the  $E2/M1$  mixing ratio of 1.15 for the 1603.7 keV transition [43], the  $B(E2)$  ratio increases to 26.

For the 2023.0 keV ( $2_4^+$ ) and 2073.7 keV  $0_4^+$  states, presumably due to the very weak population in the present decay experiment, only a decay branch to the one-phonon  $2_1^+$  state has been observed. Since the  $\Delta N=1$  transitions are disfavored by their low energies comparing with  $\Delta N=2$ , the fact that of  $\Delta N=1$  transitions are not observed from these two levels does not directly contradict the interpretation. In  $^{116}\text{Cd}$  the  $(n, n'\gamma)$  reaction measurements have shown that the  $2_4^+$  state at 1951.4 keV predominantly decays to the two-phonon  $0_2^+$  state [10,44]. In any case, further investigations are needed for a better understanding of the  $0_4^+$  and  $2_4^+$  states in  $^{118}\text{Cd}$ .

In  $^{120}\text{Cd}$ , we have pointed out that the 1899.0 keV ( $3^+$ ), 1920.5 keV ( $2_3^+$ ), 1997.9 keV ( $4_2^+$ ), and the 2032.8 keV  $6^+$  levels could be candidates for the three-phonon states. Assuming that the above spin assignments are correct, for the 1997.9 keV ( $4_2^+$ ) state, the  $B(E2; 4_2^+ \rightarrow 2_2^+)/B(E2; 4_2^+ \rightarrow 2_1^+)$  value of 77 can be deduced, which is very close to the

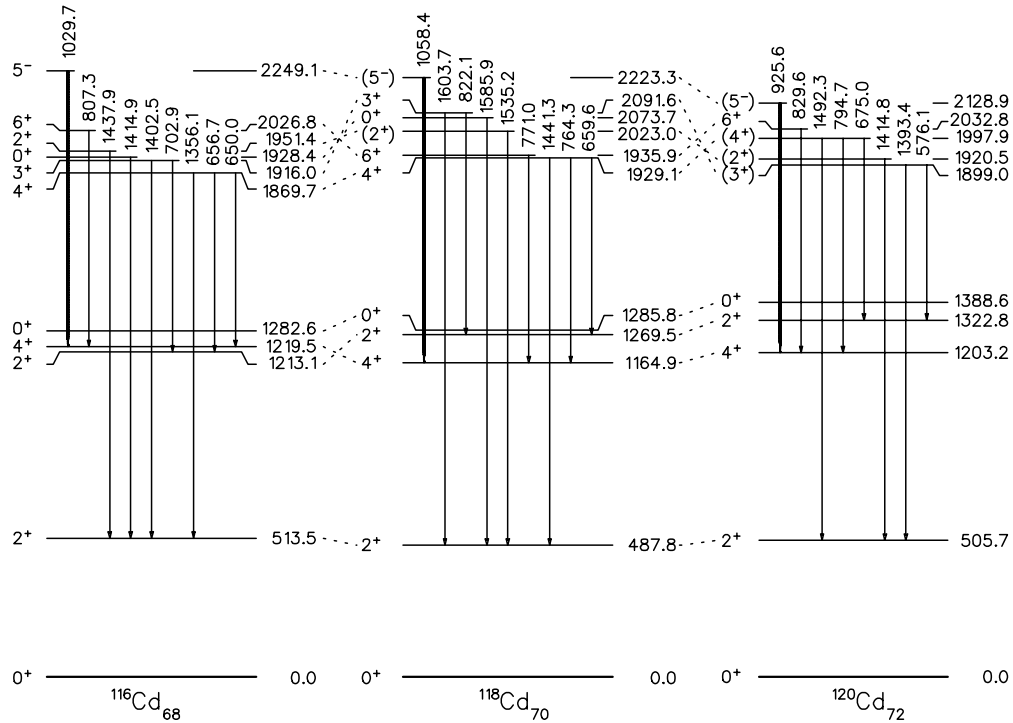


FIG. 10. Comparison of the three-phonon states in  $^{116,118,120}\text{Cd}$  populated in  $\beta^-$  decays. A  $5^-$  level mentioned in the preceding section is also shown. Results on  $^{116}\text{Cd}$  are taken from Ref. [9].

value for the 1929.1 keV  $4_2^+$  level in  $^{118}\text{Cd}$ . For the 1899.0 keV ( $3_1^+$ ) state, the  $B(E2; 3_1^+ \rightarrow 2_2^+)/B(E2; 3_1^+ \rightarrow 2_1^+)$  ratio is 51 if pure  $E2$  transitions are assumed. Finally, the three-phonon states in  $^{116,118,120}\text{Cd}$  nuclei are shown in Fig. 10 for comparison.

### C. $\beta$ -decay properties

The neutron-rich odd-odd Rh and Ag isotopes are known to have a higher-spin isomer that strongly decays to the two-quasineutron states in the even-even daughter nuclei [9,35,45,46]. According to the spherical single-particle model, the allowed Gamow-Teller transition for neutron-rich rhodium and silver nuclei is only energetically possible via a core neutron  $\nu g_{7/2} \rightarrow \pi g_{9/2}$  transition. Therefore, it can be inferred that the main component of the two-quasineutron states in Pd and Cd daughter nuclei involves a  $g_{7/2}$  neutron hole plus a valence neutron among the  $d_{5/2}$ ,  $d_{3/2}$ ,  $s_{1/2}$ , and  $h_{11/2}$  orbitals. However, when considering the residual interaction and possible deformations, this simple picture may be far from adequate.

From the systematics of neutron-rich odd-mass silver isotopes, the low-lying  $\beta$ -decaying isomers are the  $1/2^-$ ,  $7/2^-$  states [47]. Rotational bands built on top of these two levels have been established and interpreted in terms of  $\pi 1/2^- [301]$  and  $\pi 7/2^- [413]$  Nilsson orbitals associated with prolate deformations [48]. For the odd-mass Cd nuclei, one can find  $1/2^+$ ,  $3/2^+$ , and  $11/2^-$  isomers appearing at low excitation energies. It is explained that these levels might carry the major part of the neutron  $s_{1/2}$ ,  $d_{3/2}$ , and  $h_{11/2}$  strength [49]. Coupling these states, it is possible to obtain the spins of the  $\beta$ -decaying states in  $^{118}\text{Ag}$  and  $^{120}\text{Ag}$  iso-

topes. In particular, for the higher-spin isomer of  $^{118}\text{Ag}$ , spin of  $(4,5)^+$  may arise from the configurations of  $\pi 7/2^+ [413] - \nu 1/2^+ [411]$  or  $\pi 7/2^+ [413] - \nu 3/2^+ [402]$  Nilsson orbitals. In either case, Gamow-Teller transition of a core neutron in  $g_{7/2}$  orbital can lead to two-quasineutron configurations in the final state. This could correspond to the 3031.9 keV level in  $^{118}\text{Cd}$  with a low  $\log ft$  value of 4.8. In the  $^{116}\text{Ag}^m$  decay, a similar two-quasineutron state at 2958.8 keV in  $^{116}\text{Cd}$  was observed with a  $\log ft$  value of 4.9 [9]. The smoothness of the decay properties of  $^{116}\text{Ag}^m$  and  $^{118}\text{Ag}^m$  could imply very similar configurations. However, configurations must be admixed as indicated by the splitting of the GT strength over a few transitions.

In the case of  $^{120}\text{Ag}^m$ , the total strength is spread over more levels in  $^{120}\text{Cd}$ . Although the 3773.2 keV level in  $^{120}\text{Cd}$  is fed with a  $\log ft$  value of 4.8, this level is somehow higher in excitation energy. It is indeed necessary to invoke the  $h_{11/2}$  orbital to create the  $6^-$  state for  $^{120}\text{Ag}^m$ . This is found in odd-mass Cd nuclei as creating the  $11/2^-$  isomers [49].

### V. CONCLUSION

$\beta$  decays of neutron-rich  $^{118}\text{Ag}$  and  $^{120}\text{Ag}$  isotopes have been investigated using on-line mass-separated sources. The decay properties of  $^{118}\text{Ag}^m$  are similar to  $^{116}\text{Ag}^m$ , but different from  $^{120}\text{Ag}^m$ , which might indicate the onset of occupation of  $h_{11/2}$  neutron orbital. A large number of new levels in  $^{118}\text{Cd}$  and  $^{120}\text{Cd}$  has been observed. In the case of  $^{118}\text{Cd}$ , the complete set of the quadrupole three-phonon quintuplet has been presented with a new level at 2023.0 keV. A 2322.4 keV level is proposed as the  $4^+$  intruder state on top of the  $0_3^+$  and  $2_3^+$  states following the systematics. Candidates for

the quadrupole three-phonon states in  $^{120}\text{Cd}$  have been also presented. The results support the coexistence of quadrupole anharmonic vibration and intruder excitations in these two Cd nuclei. In order to test the predictions of relevant nuclear models and definitely establish the origin of excitations, further measurements of angular correlations and transition rates are highly needed.

## ACKNOWLEDGMENTS

This work has been supported by the Academy of Finland under the Finnish Center of Excellence Program 2000–2005 (Project No. 44875, Nuclear and Condensed Matter Programme at the JYFL). The authors would like to thank K. Heyde, R. Fossion, and R. Julin for valuable discussions.

- 
- [1] G. Scharff-Goldhaber and J. Weneser, Phys. Rev. **98**, 212 (1955).
- [2] D.M. Brink, A.F.R. De Toledo Piza, and A.K. Kerman, Phys. Lett. **19**, 413 (1965).
- [3] A. Bohr and B.R. Mottelson, *Nuclear Structure* (Benjamin, Reading, MA, 1975), Vol. II.
- [4] F. Corminboeuf, T.B. Brown, L. Genilloud, C.D. Hannant, J. Jolie, J. Kern, N. Warr, and S.W. Yates, Phys. Rev. Lett. **84**, 4060 (2000).
- [5] M. Délèze, S. Drissi, J. Jolie, J. Kern, and J.P. Vorlet, Nucl. Phys. **A554**, 1 (1993).
- [6] C. Fahlander, A. Bäcklin, L. Hasselgren, A. Kavka, V. Mittal, L.E. Svensson, B. Varnestig, D. Cline, B. Kotlinski, H. Grein, E. Grosse, R. Kulesa, C. Michel, W. Spreng, H.J. Wollersheim, and J. Stachel, Nucl. Phys. **A485**, 327 (1988).
- [7] R.F. Casten, J. Jolie, H.G. Börner, D.S. Brenner, N.V. Zamfir, W.-T. Chou, and A. Aprahamian, Phys. Lett. B **297**, 19 (1992).
- [8] A. Aprahamian, D.S. Brenner, R.F. Casten, R.L. Gill, and A. Piotrowski, Phys. Rev. Lett. **59**, 535 (1987).
- [9] Y. Wang, P. Dendooven, J. Huikari, A. Jokinen, V.S. Kolhinen, G. Lhersonneau, A. Nieminen, S. Nummela, H. Penttilä, K. Peräjärvi, S. Rinta-Antila, J. Szerypo, J.C. Wang, and J. Äystö, Phys. Rev. C **64**, 054315 (2001).
- [10] M.W. Kadi, Ph.D. thesis, University of Kentucky, 1998.
- [11] J. Kern, P.E. Garrett, J. Jolie, and H. Lehmann, Nucl. Phys. **A593**, 21 (1995).
- [12] K. Heyde, P. Van Isacker, M. Waroquier, G. Wenes, and M. Sambataro, Phys. Rev. C **25**, 3160 (1982).
- [13] A. Aprahamian, D.S. Brenner, R.F. Casten, R.L. Gill, A. Piotrowski, and K. Heyde, Phys. Lett. **140B**, 22 (1984).
- [14] K. Heyde, C. De Coster, J. Jolie, and J.L. Wood, Phys. Rev. C **46**, 541 (1992).
- [15] K. Heyde, C. De Coster, J.L. Wood, and J. Jolie, Phys. Rev. C **46**, 2113 (1992).
- [16] M. Délèze, S. Drissi, J. Kern, P.A. Tercier, J.P. Vorlet, J. Rik-ovska, T. Otsuka, S. Judge, and A. Williams, Nucl. Phys. **A551**, 269 (1993).
- [17] K. Heyde, J. Jolie, H. Lehmann, C. De Coster, and J.L. Wood, Nucl. Phys. **A586**, 1 (1995).
- [18] H.W. Fielding, R.E. Anderson, C.D. Zafiratos, D.A. Lind, F.E. Cecil, H.H. Wieman, and W.P. Alford, Nucl. Phys. **A281**, 389 (1977).
- [19] J. Kumpulainen, R. Julin, J. Kantele, A. Passoja, W.H. Trzaska, E. Verho, J. Väärämäki, D. Cutoiu, and M. Ivascu, Phys. Rev. C **45**, 640 (1992).
- [20] S. Juutinen, R. Julin, P. Jones, A. Lampinen, G. Lhersonneau, E. Mäkelä, M. Piiparinen, A. Savelius, and S. Törmänen, Phys. Lett. B **386**, 80 (1996).
- [21] R. Julin, Phys. Scr. **56**, 151 (1995).
- [22] N.V. Zamfir, R.L. Gill, D.S. Brenner, R.F. Casten, and A. Wolf, Phys. Rev. C **51**, 98 (1995).
- [23] J.L. Durell, in *The Spectroscopy of Heavy Nuclei*, edited by J. F. Sharpey-Schafer and L. D. Skouras, IOP Conf. Proc. No. 105 (Institute of Physics, London, 1990), p. 307.
- [24] J.H. Hamilton, A.V. Ramayya, S.J. Zhu, G.M. Ter-Akopian, Yu Ts Oganessian, J.D. Cole, J.O. Rasmussen, and M.A. Stoyer, Prog. Part. Nucl. Phys. **35**, 635 (1995).
- [25] N. Fotiades, J.A. Cizewski, K.Y. Ding, R. Krücken, J.A. Becker, L.A. Bernstein, K. Hauschild, D.P. McNabb, W. Younes, P. Fallon, I.Y. Lee, and A.O. Macchiavelli, Phys. Scr. **88**, 127 (2000).
- [26] B. Fogelberg, A. Bäcklin, and T. Nagarajan, Phys. Lett. **36B**, 334 (1971).
- [27] W. Bröchle and G. Herrmann, Radiochim. Acta **30**, 1 (1982).
- [28] K. Aleklett, P. Hoff, E. Lund, and G. Rudstam, Phys. Rev. C **26**, 1157 (1982).
- [29] A. Aprahamian, Ph.D. thesis, Clark University, 1985.
- [30] H. Mach, M. Moszynski, R.F. Casten, R.L. Gill, D.S. Brenner, J.A. Winger, W. Krips, C. Wesselborg, M. Büscher, F.K. Wohn, A. Aprahamian, D. Alburger, A. Gelberg, and A. Piotrowski, Phys. Rev. Lett. **63**, 143 (1989).
- [31] J. Äystö, Nucl. Phys. **A639**, 477 (2001).
- [32] J. Ärje, J. Äystö, H. Hyvönen, P. Taskinen, V. Koponen, J. Honkanen, A. Hautojärvi, and K. Vierinen, Phys. Rev. Lett. **54**, 99 (1985).
- [33] P. Dendooven, Nucl. Instrum. Methods Phys. Res. B **126**, 182 (1997).
- [34] H. Penttilä, P. Dendooven, A. Honkanen, M. Huhta, P.P. Jauho, A. Jokinen, G. Lhersonneau, M. Oinonen, J.-M. Parmonen, K. Peräjärvi, and J. Äystö, Nucl. Instrum. Methods Phys. Res. B **126**, 213 (1997).
- [35] Y. Wang, P. Dendooven, J. Huikari, A. Jokinen, V.S. Kolhinen, G. Lhersonneau, A. Nieminen, S. Nummela, H. Penttilä, K. Peräjärvi, S. Rinta-Antila, J. Szerypo, J.C. Wang, and J. Äystö, Phys. Rev. C **63**, 024309 (2001).
- [36] H. Penttilä, J. Äystö, P. Jauho, A. Jokinen, J.M. Parmonen, P. Taskinen, K. Eskola, M. Leino, P. Dendooven, and C.N. Davids, Phys. Scr. **32**, 38 (1990).
- [37] Z. Janas, J. Äystö, K. Eskola, P.P. Jauho, A. Jokinen, J. Kownacki, M. Leino, J.M. Parmonen, H. Penttilä, J. Szerypo, and J. Zylicz, Nucl. Phys. **A552**, 340 (1993).
- [38] V. Koponen, J. Äystö, J. Honkanen, P. Jauho, H. Penttilä, J. Suhonen, P. Taskinen, K. Rykaczewski, J. Zylicz, and C.N. Davids, Z. Phys. A **333**, 339 (1989).
- [39] A. Savelius, Ph.D. thesis, University of Jyväskylä, 1998.
- [40] N. Buforn, A. Astier, J. Meyer, M. Meyer, S. Perriès, N. Re-

- don, O. Stézowski, M.G. Porquet, I. Deloncle, A. Bauchet, J. Duprat, B.J.P. Gall, C. Gautherin, E. Gueorguieva, F. Hoellinger, T. Kutsarova, R. Lucas, A. Minkova, N. Schulz, H. Sergolle, Ts. Venkova, and A.N. Wilson, *Eur. Phys. J. A* **7**, 347 (2000).
- [41] K. Fransson, M. AF Ugglas, and Å. Engström, *Nucl. Instrum. Methods* **113**, 157 (1973).
- [42] P.L. Reeder, R.A. Warner, and R.L. Gill, *Phys. Rev. C* **27**, 3002 (1983).
- [43] R.B. Firestone *et al.*, *Table of Isotopes*, 8th ed. (Wiley, New York, 1996).
- [44] S.Y. Araddad, A.M. Demidov, S.M. Zleetni, V.A. Kurkin, and J.M. Rateb, *Sov. J. Nucl. Phys.* **54**, 181 (1991).
- [45] J. Äystö, C.N. Davids, J. Hattula, J. Honkanen, K. Honkanen, P. Jauho, R. Julin, S. Juutinen, J. Kumpulainen, T. Lönnroth, A. Pakkanen, A. Passoja, H. Penttilä, P. Taskinen, E. Verho, A. Virtanen, and M. Yoshii, *Nucl. Phys.* **A480**, 104 (1988).
- [46] G. Lhersonneau, J.C. Wang, S. Hankonen, P. Dendooven, P. Jones, R. Julin, and J. Äystö, *Phys. Rev. C* **60**, 014315 (1999).
- [47] H. Penttilä, J. Äystö, K. Eskola, Z. Janas, P.P. Jauho, A. Jokinen, M.E. Leino, J.M. Parmonen, and P. Taskinen, *Z. Phys. A* **338**, 291 (1991).
- [48] J.K. Hwang, A.V. Ramayya, J.H. Hamilton, C.J. Beyer, X.Q. Zhang, J.O. Rasmussen, Y.X. Luo, S.C. Wu, T.N. Ginter, I.Y. Lee, C.M. Folden, P. Fallon, P. Zielinski, K.E. Gregorich, A.O. Macchiavelli, M.A. Stoyer, and S.J. Asztalos, *Phys. Rev. C* **65**, 054314 (2002).
- [49] B. Fogelberg and P. Hoff, *Nucl. Phys.* **A391**, 445 (1982).